Journal of Photochemistry and Photobiology A: Chemistry 218 (2011) 101–110

Contents lists available at ScienceDirect

Journal of Photochemistry and Photobiology A: Chemistry

journal homepage: www.elsevier.com/locate/jphotochem

The determination of the photosensitizing properties of mercapto substituted phthalocyanine derivatives in the presence of quantum dots capped with mercaptopropionic acid

Sharon Moeno, Edith Antunes, Tebello Nyokong*

Department of Chemistry, Rhodes University, P.O. Box 94, Grahamstown 6140, South Africa

ARTICLE INFO

Article history:
Received 29 September 2010
Received in revised form
29 November 2010
Accepted 9 December 2010
Available online 16 December 2010

Keywords:
Metallophthalocyanine
Mercaptoacetic acid
Mercaptopropionic acid
Fluorescence quantum yield

ABSTRACT

This work reports on the synthesis of several novel water soluble metallophthalocyanines containing Zn^{2+}, In^{3+}, Ga^{3+} or Si^{4+} as central metal ions and tetra substituted with mercaptoacetic acid and mercaptopropionic acid. The complexes were characterized using infra red, nuclear magnetic resonance and mass spectroscopies as well as elemental analysis. All the complexes are water soluble but the majority are highly aggregated in water and organic solvents. The complex containing Zn as a central metal and mercaptopropionic acid as a substituent was not aggregated allowing for the determination of photophysical parameters. This complex had triplet state quantum yield of 0.61 in DMF and 0.88 in DMSO while the fluorescence quantum yield was 0.13 in DMSO. The determination of photophysical properties of the complex containing Zn as a central metal and mercaptopropionic acid were carried out in the presence of mercaptopropionic acid capped CdTe quantum dots. There is an increase in triplet state quantum yield from 0.88 (for the phthalocyanine alone) to 0.94 (in the presence of CdTe quantum dots) in DMSO.

1. Introduction

Metallophthalocyanines (MPcs) are versatile and highly stable complexes. They have varied applications, but the use of these complexes as photosensitizers for photodynamic therapy (PDT) of cancer in medicine has gained momentum [1–5]. This is because they show exceptional properties that contribute towards their efficiency in cancer therapy [1–6].

The inclusion of closed shell metal ions (such as zinc, aluminium and silicon) in the cavity of the phthalocyanine (Pc) ring results in complexes with desirable photophysical properties such as high triplet state quantum yields and long triplet lifetimes [7,8]. These properties are a prerequisite for efficient photosensitization in PDT. PDT involves favoured accumulation of the MPc at the targeted tumour tissue followed by selective illumination of the target area with near infrared light. The red light is able to penetrate the skin and cause excitation of the MPc in the tumour tissue [9–11].

In the event that the photosensitizer molecules reach the triplet state through intersystem crossing they may transfer their triplet state energy to nearby ground state oxygen resulting in excited and highly reactive singlet oxygen species which is responsible for the necrosis of the tumour tissue [1–3]. Although water soluble MPcs tend to be aggregated in aqueous media they are favoured for PDT purposes because they can easily be administered into the blood stream.

Advances in cancer therapy have led to the exploitation of imaging and tagging tools. Semiconductor nanoparticles are rapidly gaining recognition in this regard. These nanoparticles also known as quantum dots (QDs) possess excellent size tuneable optical properties, high photostability and high photoluminescence quantum yields [12,13]. It is for these reasons that the use of QDs in PDT for imaging purposes has escalated [14,15]. When the fluorophores of QDs are in close proximity to the acceptor (photosensitizer) molecule fluorophores and under condusive conditions, non-radiative transfer of energy from the donor (QDs) to the acceptor molecules may take place. This transfer of energy is referred to as Förster resonance energy transfer (FRET) [16–19].

Our group has recently [20] reported on FRET between octa carboxy phthalocyanines (which are negatively charged) and quantum dots (also negatively charged) where it was found that an efficient energy transfer process from the latter to the former occurred. We have also observed that positively charged ZnPc containing sulfur linkages did not show FRET, while those containing oxygen bridges showed FRET [21]. Positively charged zinc porphyrazine underwent reduction in the presence of QDs [22]. In this work we study the

* Corresponding author. Tel.: +27 46 6038260; fax: +27 46 6225109.
E-mail address: t.nyokong@ru.ac.za (T. Nyokong).

1010-6030/$ – see front matter © 2010 Elsevier B.V. All rights reserved.
doi:10.1016/j.jphotochem.2010.12.009

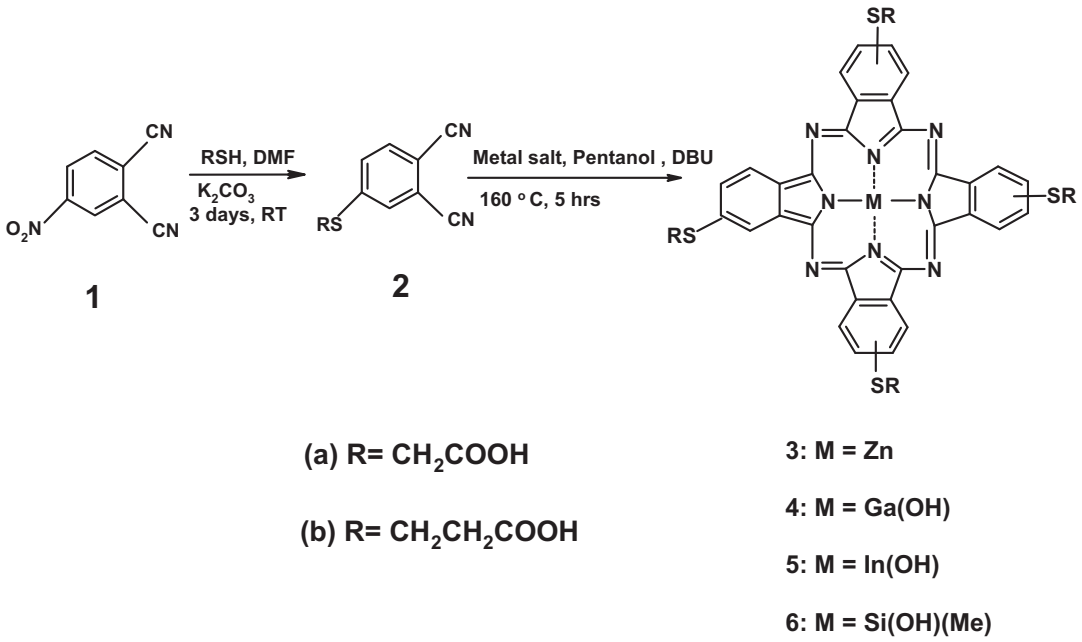

Scheme 1. Synthetic route of mercaptoacetic acid and mercaptopropanoic acid tetra substituted metallophthalocyanine complexes.

behaviour of negatively charged ZnPcs containing sulfur linkages in the presence of QDs. MPc complexes containing carboxylic groups and also bridged with sulfur groups are rare [23], hence this work presents the synthesis of new water soluble and tetra peripherally substituted Pcs with Zn^{2+}, Ga^{3+}, In^{3+} and Si^{4+} as central metal ions with mercaptoacetic acid (a) and mercaptopropionic acid (b) substituents respectively (complexes **3**–**6**, Scheme 1).

2. Experimental

2.1. Materials

2-Mercaptopropionic acid (MPA) 98%, zinc acetate dihydrate, 4-nitrophthalic acid, 1-pentanol, ZnPc, and zinc tetrasulfophthalocyanine (ZnTSPc) were obtained from Sigma–Aldrich. Potassium carbonate, ethanol, diethylether, acetone, gallium chloride, indium chloride, chlorotrimethylsilane, tetrahydrofuran (THF) and sodium hydroxide were obtained from Saarchem. Dimethyl sulphoxide (DMSO), anthracene-9,10-bis-methylmalonate (ADMA) and 1,8-diazabicyclo[5,4,0]undec-7-ene (DBU) were obtained from Fluka. Ultra pure water was obtained from a Milli-Q Water System (Millipore Corp., Bedford, MA, USA). The surfactant Triton X-100 (Aldrich) was employed in order to reduce the aggregated nature of the phthalocyanine complexes in aqueous media. 3-Mercaptopropionic acid (MPA) capped CdTe QDs (MPA–CdTe QDs) were synthesized, purified and characterized according to the literature [24,25]. The size of MPA–CdTe QDs used in this work is 4.1 nm. For FRET studies (for **3b**) an ethanol: 0.01 M NaOH (1:1) solvent mixture was employed to monomerize the complex. The rest of the complexes could not be monomerized by this solvent mixture.

2.2. Synthesis

2.2.1. ZnPc derivatives

*2.2.1.1. 4-(2-Mercaptoacetic acid) phthalonitrile (**2a**, Scheme 1).* 2-Mercaptoacetic acid (1.93 g, 21 mmol) and 4-nitrophthalonitrile (3.63 g, 21 mmol) were dissolved in DMF (80 mL) under a stream of nitrogen and the mixture stirred at room temperature for 15 min. Thereafter, finely ground K_2CO_3 (4.5 g, 33 mmol) was added portion wise over a period of 4 h and the reaction mixture left to stir for a further 72 h at room temperature. The mixture was then added to diethyl ether (150 mL) and stirred for 15 min. The resulting precipitate was filtered off, thoroughly washed with diethyl ether and acetone, dried and recrystallized from an ethanol:chloroform mixture (5:1). Yield: 10.1 g (93%). IR [(KBr) ν_{max}/cm^{-1}]: 3397 (ν_{COOH}), 2222 ($\nu_{C\equiv N}$), 1641–1603 ($\nu_{C=C}$), 1448–1381 (ν_{C-OH}), 1310–1113 (ν_{C-O}), 910–827 (ν_{C-S-C}). ^{1}H NMR (600 MHz), DMSO-d_6 δ ppm: 10.01 (m, 1H, Carboxyl-H), 7.92 (d, 1H, Ar–H), 7.89 (d, 1H, Ar–H), 7.66 (dd, 1H, Ar–H), 3.71 (m, 2H, methine-H).

*2.2.1.2. 4-(2-Mercaptopropionic acid) phthalonitrile (**2b**, Scheme 1).* The synthesis for **2b** was the same as for **2a** except 2-mercaptopropionic acid (2.2 g, 21 mmol) was employed instead of 2-mercaptoacetic acid. The amounts of the reagents were the same as for **2a**. Yield: 10.7 g (92%). IR [(KBr) ν_{max}/cm^{-1}]: 3324 (ν_{COOH}), 2263 ($\nu_{C\equiv N}$), 1664–1582 ($\nu_{C=C}$), 1455–1380 (ν_{C-OH}), 1331–1274 (ν_{C-O}) 880–803 (ν_{C-S-C}). ^{1}H NMR (600 MHz), DMSO-d_6 δ ppm: 9.91(s, 1H, Carboxyl-H), 7.98 (d, 1H, Ar–H), 7.71 (dd, 1H, Ar–H), 7.64 (d, 1H, Ar–H), 3.41 (m, 2H, methine-H), 3.21 (m, 2H, methine-H).

*2.2.1.3. 2,(3)-[Tetra-(mercaptoacetic acid phthalocyaninato) zinc(II)] (**3a**, Scheme 1).* A mixture of anhydrous zinc(II) acetate (0.51 g, 2.8 mmol), 4-(mercaptoacetic acid) phthalonitrile (**2a**) (0.50 g, 2.34 mmol), DBU (0.55 mL, 4 mmol) and pentanol (15 mL) was stirred at 160 °C for 5 h. After cooling, the solution was mixed with *n*-hexane. The green solid product was precipitated and collected by filtration and washed with *n*-hexane. The crude product was purified with chloroform, acetone and ethanol. The phthalocyanine was then dissolved in 5 mL of 0.1 M NaOH solution and precipitation of the product from solution was achieved with the use of (100 mL) of 20% HCl solution and this was repeated several times and the product was finally dissolved in THF and left to dry. Yield: 0.019 g (5%) UV/Vis (0.01 M NaOH): λ_{max} (nm); 692, 628, 351. IR [(KBr) ν_{max}/cm^{-1}]: 3444 (ν_{COOH}), 1662 ($\nu_{C=C}$), 1437–1407 (ν_{C-OH}), 698 (ν_{C-S-C}). ^{1}H NMR (600 MHz, DMSO-d_6) δ ppm: 8.34 (m, 4H, Carboxyl-H), 7.84–7.06 (m, 8H, Ar–H), 6.88 (s, 4H, Ar–H), 4.25 (m, 8H, Methyl-H). Calc. for $C_{40}H_{24}N_8S_4O_8Zn$: C, 51.20; H, 2.70; N, 12.61; S, 14.42. Found: C, 50.98; H, 2.99; N, 11.89; S, 13.61. MALDI-TOF-MS *m/z*: Calc.: 938.29. Found: 940.09 $[M+2]^+$ for $C_{40}H_{24}N_8S_4O_8Zn$.

*2.2.1.4. 2,(3)-[Tetra-(mercaptoacetic acid phthalocyaninato) gallium(III)](OH) (**4a**, Scheme 1).* The method employed for synthesis and purification of **4a** was the same as the one used for **3a** except anhydrous gallium(III) chloride (0.49 g, 2.8 mmol) was used as metal salt. The amounts of all the reagents were the same as those used for **3a**. Yield: 0.11 g (20%) UV/Vis (0.01 M NaOH): λ_{max} (nm) ($\log \varepsilon$); 684, 640, 334. IR [(KBr) ν_{max}/cm^{-1}]: 3457 (ν_{COOH}), 1708 ($\nu_{C=C}$), 1436–1407 (ν_{C-OH}), 697 (ν_{C-S-C}). ^{1}H NMR (600 MHz, DMSO-d_6) δ ppm: 9.49 (m, 4H, Carboxyl-H), 8.18 (m, 8H, Ar–H), 6.87 (s, 4H, Ar–H), 4.22 (m, 8H, Methine-H). Calc. for $C_{40}H_{24}N_8S_4O_8Ga{\cdot}OH{\cdot}3H_2O$: C, 50.07; H, 2.50; N, 11.68; S, 13.35. Found: C, 49.85; H, 3.03; N, 12.25; S, 13.31. MALDI-TOF-MS *m/z*: Calc.: 959.63. Found: 962.23 $[M+2]^+$ for $C_{40}H_{24}N_8S_4O_8Ga{\cdot}OH$.

*2.2.1.5. 2,(3)-[Tetra-(mercaptoacetic acid phthalocyaninato) indium(III)](OH) (**5a**, Scheme 1).* The method employed for synthesis and purification of **5a** was the same as the one used for **3a** except anhydrous indium(III)chloride (0.62 g, 2.8 mmol) was used as metal salt. The amounts of all the reagents were the same as those used for **3a**. Yield: 0.065 g (12%) UV/Vis (0.01 M NaOH): λ_{max} (nm); 689, 653, 349. IR [(KBr) ν_{max}/cm^{-1}]: 3451 (ν_{COOH}), 1697 ($\nu_{C=C}$), 1436 (ν_{C-OH}), 697 (ν_{C-S-C}). ^{1}H NMR (600 MHz, DMSO-d_6) δ ppm: 9.32 (m, 4H, Carboxyl-H), 7.89 (m, 8H, Ar–H), 6.88 (s, 4H, Ar–H), 4.33 (m, 8H, Methyl-H). Calc. for $C_{40}H_{24}N_8S_4O_8In{\cdot}OH(THF)$: C, 49.09; H, 2.99; N, 10.41; S, 11.91. Found: C, 49.17; H, 2.42; N, 9.86; S, 11.98. MALDI-TOF-MS *m/z*: Calc.: 1004.7. Found: 1006.19 $[M+1]^+$ for $C_{40}H_{24}N_8S_4O_8In{\cdot}OH$.

*2.2.1.6. 2,(3)-[Tetra-(mercaptoacetic acid phthalocyaninato) silicon (IV)](OH)(Me) (**6a**, Scheme 1).* The method employed for synthesis and purification of **6a** was the same as the one used for **3a** except chlorotrimethylsilane(IV) (0.38 g, 2.8 mmol) was used as metal source. The amounts of all the reagents were the same as those used for **3a**. Yield: 0.05 g (10%) UV/Vis (0.01 M NaOH): λ_{max} (nm); 685, 645, 340. IR [(KBr) ν_{max}/cm^{-1}]: 3459 (ν_{COOH}), 1709 ($\nu_{C=C}$), 1436 (ν_{C-OH}), 697 (ν_{C-S-C}). ^{1}H NMR (600 MHz, DMSO-d_6) δ ppm: 8.02–7.78 (m, 4H, Carboxyl-H), 7.41–7.04 (m, 8H, Ar–H), 6.93(m, 4H, Ar–H), 3.99–3.97 (m, 8H, Methine-H). Calc. for $C_{40}H_{24}N_8S_4O_8Si{\cdot}(OH)(Me)$: C, 51.38; H, 2.68; N, 11.99; S, 13.70. Found: C, 52.51; H, 2.94; N, 10.74; S, 14.10. MALDI-TOF-MS *m/z*: Calc.: 933.08. Found: 934.63 $[M+2]^+$ for $C_{40}H_{24}N_8S_4O_8Si{\cdot}(OH)(Me)$.

*2.2.1.7. 2,(3)-[Tetra-(mercaptopropanoic acid phthalocyaninato) zinc(II)] (**3b**, Scheme 1).* The method employed for synthesis of **3b** was the same as the one used for **3a** except compound **2b** was employed instead of **2a**. The amounts of all the reagents were the same as those used for **3a**. Yield: 0.38 g (72%) UV/Vis (0.01 M NaOH:methanol): λ_{max} (nm) ($\log \varepsilon$); 693 (3.98), 628 (3.64), 353 (4.11). IR [(KBr) ν_{max}/cm^{-1}]: 3452 (ν_{COOH}), 1709 ($\nu_{C=C}$), 1436–1407 (ν_{C-OH}), 697 (ν_{C-S-C}). ^{1}H NMR (600 MHz, DMSO-d_6) δ ppm: 8.80 (m, 4H, Carboxyl-H), 8.01 (m, 8H, Ar–H), 6.87 (s, 4H, Ar–H), 2.65 (m, 16H, Methine-H). Calc. for $C_{44}H_{32}N_8S_4O_8Zn{\cdot}3H_2O$: C, 50.40; H, 3.62; N, 10.69; S, 12.21. Found: C, 50.54; H, 2.65; N, 10.04; S, 13.32. MALDI-TOF-MS *m/z*: Calc.: 994.44. Found: 995.3 $[M+1]^+$ for $C_{44}H_{32}N_8S_4O_8Zn$.

*2.2.1.8. 2,(3)-[Tetra-(mercaptopropionic acid phthalocyaninato) gallium(III)](OH) (**4b**, Scheme 1).* The method employed for synthesis of **4b** was the same as the one used for **3a** except anhydrous gallium(III) chloride (0.49 g, 2.8 mmol) was used as metal salt, and compound **2b** was employed instead of **2a**. The amounts of all the other reagents were the same as those used for **3a**. Yield: 0.017 g (5%) UV/Vis (0.01 M NaOH): λ_{max} (nm); 687, 650, 345. IR [(KBr) ν_{max}/cm^{-1}]: 3449 (ν_{COOH}), 1709 ($\nu_{C=C}$), 1437–1407 (ν_{C-OH}), 697 (ν_{C-S-C}). ^{1}H NMR (600 MHz, DMSO-d_6) δ ppm: 7.99 (m, 4H, Carboxyl-H), 7.72–7.53 (m, 8H, Ar–H), 6.86 (s, 4H, Ar–H), 2.92 (m, 16H, Methine-H). Calc. for $C_{44}H_{32}N_8S_4O_8Ga{\cdot}OH{\cdot}2H_2O$: C, 50.24; H, 3.45; N, 10.66; S, 12.19. Found: C, 50.68; H, 2.38; N, 10.28; S, 13.97. MALDI-TOF-MS *m/z*: Calc.: 1015.79. Found: 1016.23 $[M]^+$ for $C_{44}H_{32}N_8S_4O_8Ga{\cdot}OH$.

*2.2.1.9. 2,(3)-[Tetra-(mercaptopropionic acid phthalocyaninato) indium(III)](OH) (**5b**, Scheme 1).* The method employed for synthesis of **5b** was the same as the one used for **3a** except anhydrous indium(III) chloride (0.62 g, 2.8 mmol) was used as metal salt, and compound **2b** was employed instead of **2a**. The amounts of all the reagents were the same as those used for **3a**. Yield: 0.015 g (5%) UV/Vis (0.01 M NaOH): λ_{max} (nm); 689, 651. IR [(KBr) ν_{max}/cm^{-1}]: 3450 (ν_{COOH}), 1709 ($\nu_{C=C}$), 1437 (ν_{C-OH}), 697 (ν_{C-S-C}). ^{1}H NMR (600 MHz, DMSO-d_6) δ ppm: 7.99–7.92 (m, 4H, Carboxyl-H), 7.71–7.65 (d, 8H, Ar–H), 6.86 (s, 4H, Ar–H), 2.92 (m, 16H, Methine-H). Calc. for $C_{44}H_{32}N_8S_4O_8In{\cdot}OH{\cdot}2H_2O$: C, 49.82; H, 3.14; N, 10.56; S, 12.09. Found: C, 48.26; H, 3.36; N, 10.24; S, 11.72. MALDI-TOF-MS *m/z*: Calc.: 1060.89. Found: 1062.21 $[M+1]^+$ for $C_{44}H_{32}N_8S_4O_8In{\cdot}OH$.

*2.2.1.10. 2,(3)-[Tetra-(mercaptopropionic acid phthalocyaninato) silicon(IV)](OH)(Me) (**6b**, Scheme 1).* The method employed for synthesis of **6b** was the same as the one used for **3a** except chlorotrimethylsilane(IV) (0.39 g, 2.8 mmol) was used as metal source, and compound **2b** was employed instead of **2a**. The amounts of all the reagents were the same as those used for **3a**. Yield: 0.11 g (19.4%) UV/Vis (0.01 M NaOH): λ_{max} (nm); 692, 644, 345. IR [(KBr) ν_{max}/cm^{-1}]: 3445 (ν_{COOH}), 1707 ($\nu_{C=C}$), 1437 (ν_{C-OH}), 698 (ν_{C-S-C}). ^{1}H NMR (600 MHz, DMSO-d_6) δ ppm: 7.52 (m, 4H, Carboxyl-H), 7.18–7.08 (m, 8H, Ar–H), 7.00 (s, 4H, Ar–H), 4.05 (m, 16H, Methine-H). Calc. for $C_{44}H_{32}N_8S_4O_8Si{\cdot}(OH)(Me){\cdot}2H_2O$: C, 51.55; H, 3.54; N, 10.93; S, 12.51. Found: C, 52.64; H, 3.66; N, 9.71; S, 13.10. MALDI-TOF-MS *m/z*: Calc.: 989.18. Found: 990.61 $[M+1]^+$ for $C_{44}H_{32}N_8S_4O_8Si{\cdot}(OH)(Me)$.

2.3. Photophysical and photochemical studies

2.3.1. Fluorescence and triplet state quantum yield determinations

Fluorescence quantum yields (Φ_F) were determined by a comparative method [26] using Eq. (1):

$$\Phi_F = \Phi_{F(Std)} \frac{F \cdot A_{Std} \cdot n^2}{F_{Std} \cdot A \cdot n_{Std}^2} \quad (1)$$

where F and F_{Std} are the areas under the fluorescence curves of the MPc derivatives and the reference, respectively. A and A_{Std} are the absorbances of the sample and reference at the excitation wavelength, and n and n_{Std} are the refractive indices of solvents used for the sample and standard, respectively. ZnPc in DMSO was used as a standard, $\Phi_F = 0.20$ [27] for the determination of fluorescence quantum yields of the MPc complexes in DMSO. The fluorescence quantum yields (Φ_F) of the phthalocyanine complexes are represented as $\Phi_{F(MPc)}$ (where MPc represents complexes **3**–**6**). Rhodamine 6G in ethanol with $\Phi_F = 0.94$ was employed as the standard for the quantum dots [28,29]. The sample and the standard were both excited at the same relevant wavelength. The fluorescence quantum yields of the QDs are represented as $\Phi_{F(QD)}$ where QD represents MPA capped CdTe QDs. The fluorescence quantum yield values of the QDs were employed in determining their fluorescence quantum yields in the mixture ($\Phi_{F(QD)}^{Mix}$) with complex **3b** (the only complex not affected by aggregation), Eq. (2):

$$\Phi_{F(QD)}^{Mix} = \Phi_{F(QD)} \frac{F_{QD}^{Mix}}{F_{QD}} \quad (2)$$

where $\Phi_{F(QD)}$ is the fluorescence quantum yield of the QDs alone, and was used as standard, F_{QD}^{Mix} is the fluorescence intensity of QDs in the mixture (with **3b**) when excited at the excitation wavelength of the QDs (500 nm) and F_{QD} is the fluorescence intensity of the QD alone at the same excitation wavelength.

Triplet state quantum yields were determined using a comparative method [30], using Eq. (3):

$$\Phi_T^{Sample} = \Phi_T^{Std} \frac{\Delta A_T^{Sample} \cdot \varepsilon_T^{Std}}{\Delta A_T^{Std} \cdot \varepsilon_T^{Sample}} \quad (3)$$

where ΔA_T^{Sample} and ΔA_T^{Std} are the changes in the triplet state absorbance of complex **3b** (the only un-aggregated complex) derivative and the standard, respectively. ε_T^{Sample} and ε_T^{Std} are the triplet state extinction coefficients for **3b** and the standard, respectively. Φ_T^{Std} is the triplet state quantum yield for zinc tetrasulfophthalocyanine (ZnTSPc) used as standard in aqueous solution, $\Phi_T^{Std} = 0.56$ [31] and ZnPc as standard, $\Phi_T^{Std} = 0.65$ [32] in DMSO and ZnPc $\Phi_T^{Std} = 0.58$ [33] in DMF. The triplet state quantum yields of **3b** were also determined in the mixture of QDs and are represented as $\Phi_{T(ZnPc)}^{Mix}$ and the corresponding triplet lifetimes as $\tau_{T(ZnPc)}^{Mix}$.

Quantum yields of internal conversion (Φ_{IC}) were obtained from Eq. (4). This equation assumes that only three processes (fluorescence, intersystem crossing and internal conversion), jointly deactivate the excited singlet state of the ZnPc derivatives.

$$\Phi_{IC} = 1 - (\Phi_F + \Phi_T) \quad (4)$$

2.3.2. Singlet oxygen quantum yields

The singlet oxygen quantum yield (Φ_Δ) determinations for **3b** were carried out using an experimental set-up that is described in detail elsewhere [34]. In this work Φ_Δ values were determined using DPBF as a singlet oxygen quencher in organic media [35] and ADMA in aqueous media, employing Eq. (5) for calculations of the Φ_Δ values:

$$\Phi_\Delta = \Phi_\Delta^{Std} \frac{W_{DPBF} \cdot I_{abs}^{Std}}{W_{DPBF}^{Std} \cdot I_{abs}} \quad (5)$$

where Φ_Δ^{Std} is the singlet oxygen quantum yield for the standard, (ZnPc $\Phi_\Delta^{Std} = 0.67$ in DMSO [36], ZnPc $\Phi_\Delta^{Std} = 0.56$ in DMF [37] and ZnPcSmix $\Phi_\Delta^{Std} = 0.45$ in aqueous media [38]. W_{DPBF} and W_{DPBF}^{Std} are the DPBF photobleaching rates in the presence of the ZnPc derivative under investigation and the respective standards. I_{abs} and I_{abs}^{Std} are the rates of light absorption by the ZnPc derivatives and the standard, respectively. The initial DPBF (or ADMA) concentrations used were kept the same for both the ZnPc derivatives and the respective standards.

The values of the fraction of the excited triplet state quenched by ground state molecular oxygen (S_Δ) were determined by employing Eq. (6):

$$S_\Delta = \frac{\Phi_\Delta}{\Phi_T} \quad (6)$$

2.4. Determination of FRET parameters

Förster resonance energy transfer (FRET) is a non-radiative energy transfer from a photoexcited donor fluorophore, to an acceptor fluorophore of a different species which is in close proximity. This energy transfer is mainly dependent on: the center-to-center separation distance between donor and acceptor (r), the degree of spectral overlap of the donor's fluorescence emission spectrum and the acceptor's absorption spectrum (J) and the orientation of the donor and acceptor transition dipoles [16,29]. The occurrence of FRET is evidenced by a decrease of the donor photoemission accompanied by an increase in the acceptor's fluorescence. The FRET efficiency (Eff) is determined experimentally from the fluorescence quantum yields of the donor in the absence ($\Phi_{F(QD)}$) and presence ($\Phi_{F(QD)}^{Mix}$) of the acceptor using Eq. (7) [16,29]:

$$Eff = 1 - \frac{\Phi_{F(QD)}^{Mix}}{\Phi_{F(QD)}} \quad (7)$$

The FRET efficiency was also determined using average fluorescence lifetimes of the donor (MPA QDs) in the presence of (τ_{DA}) and the absence (τ_D) of the acceptor (**3b**) using Eq. (8):

$$Eff = 1 - \frac{\tau_{DA}}{\tau_D} \quad (8)$$

The efficiency of energy transfer (Eff) is related to r (Å) by Eq. (9) [29]:

$$Eff = \frac{R_0^6}{R_0^6 + r^6} \quad (9)$$

where R_0 (the Förster distance, Å) is the critical distance between the donor and acceptor fluorophores at which the efficiency of energy transfer is 50%. R_0 depends on the quantum yield of the donor, Eq. (10) [29]:

$$R_0^6 = 8.8 \times 10^{23} \kappa^2 n^{-4} \Phi_{F(QD)} J \quad (10)$$

where n is the refractive index of the medium; Φ_F is the fluorescence quantum yield of the donor in the absence of the acceptor; J is the Förster overlap integral and κ^2 is the transition dipole orientation factor. In this case, it is assumed that κ^2 is 2/3. This assumption is often made for donor–acceptor pairs in a liquid medium. FRET parameters were computed using the program PhotochemCAD [39]. J, the Förster overlap integral, is defined by Eq. (11):

$$J = \int f_{QD}(\lambda) e_{ZnPc}(\lambda) \lambda^4 \, \partial\lambda \quad (11)$$

where f_{QD} is the normalized QD emission spectrum; ε_{ZnPc} is the molar extinction coefficient of the ZnPc derivative; and λ is the wavelength of the acceptor (the Q band).

2.5. Equipment

Fluorescence excitation and emission spectra were recorded on a Varian Eclipse spectrofluorimeter. UV–Vis spectra were recorded on a Varian 500 UV–Vis/NIR spectrophotometer. IR data were obtained by using the Perkin-Elmer spectrum 2000 FTIR spectrometer. ^{1}H NMR spectra were recorded using a Bruker AMX 400 MHz spectrometer. Elemental analyses were carried out on a Vario EL III MicroCube CHNS Analyzer.

Fluorescence lifetimes were measured using a time correlated single photon counting (TCSPC) setup (FluoTime 200, Picoquant GmbH). The excitation source for MPA–CdTe QDs was a diode laser (LDH-P-C-485 with 10 MHz repetition rate, 88 ps pulse width) and the time resolved emission spectroscopy (TRES) measurements of the MPc complexes were obtained using a different diode laser (LDH-P-670 with PDL 800-B, Picoquant GmbH, 670 nm, 20 MHz repetition rate, 44 ps pulse width) at steps of 4 nm. Fluorescence was detected under the magic angle with a peltier cooled photomultiplier tube (PMT) (PMA-C 192-N-M, Picoquant) and integrated electronics (PicoHarp 300E, Picoquant GmbH). A monochromator with a spectral width of about 8 nm was used to select the required emission wavelength band. The response function of the system, which was measured with a scattering Ludox solution (DuPont), had a full width at half-maximum (FWHM) of about 300 ps. The ratio of stop to start pulses was kept low (below 0.05) to ensure good statistics. All luminescence decay curves were measured at the maximum of the emission peak. The data were analysed with

the program FluoFit (Picoquant). The support plane approach was used to estimate the errors of the decay times [29]. Mass spectra data were collected with a Bruker AutoFLEX III Smartbeam TOF/TOF Mass spectrometer. The instrument was operated in positive ion mode using an m/z range of 400–3000. The voltage of the ion sources were set at 19 and 16.7 kV for ion sources 1 and 2, respectively, while the lens were set at 8.50 kV. The reflector 1 and 2 voltages were set at 21 and 9.7 kV, respectively. The spectra were acquired using dithranol as the MALDI matrix, using a 354 nm Nd:YAG laser.

3. Results and discussion

The new complexes (**3**–**6**) were characterized by UV–Vis, IR, NMR spectroscopies, MALDI-TOF mass spectra and elemental analysis. All the analyses are consistent with the expected results as shown in Section 2. The complexes exhibited moderate solubility in organic solvents such as DMF and DMSO as well as in aqueous solution.

The mass spectra of the phthalocyanines were obtained by the relatively soft ionization MALDI-TOF technique with the molecular ion peaks observed at m/z 940.09 (**3a**), 995.3 (**3b**), 962.23 (**4a**), 1016.23 (**4b**), 1006.19 (**5a**), 1062 (**5b**), 934. 63 (**6a**) and 990.61 for **6b** as shown in Section 2. Hydroxyl as axial ligands are expected due to the use of sodium hydroxide solution during the purification process.

As expected the synthesis of the tetra substituted MPcs resulted in the formation of four different isomers which are obtained in an expected statistical mixture, however no attempt was made to separate the isomer mixtures of the MPc complexes. The four probable isomers can be designed by their molecular symmetry as C_{4h}, C_{2v}, C_s and D_{2h}. The peripherally tetra-substituted compounds always occur in the expected statistical mixture of 12.5% C_{4h}-, 25% C_{2v}-, 50% C_s- and 12.5% D_{2h}-isomer [23]. The ^{1}H NMR spectra of phthalocyanine derivatives (**3**–**6**) show complex patterns due to the mixed isomer character of these compounds, and due to aggregation. However, the complexes were found to be pure by ^{1}H NMR with all the substituents and ring protons observed in their respective regions. Due to the broad nature of the ^{1}H NMR spectra, signals due to axial ligands (for complexes **4**–**6**, containing axial ligands) were not observed. Hydrogen bonding will also affect the ^{1}H NMR spectra since the MPc complexes have substituents with terminal carboxyl moieties and complexes **4**–**6** have hydroxyl axial ligands. However, mass spectra and elemental analyses confirmed the formation of the complexes. Due to aggregation, the determination of extinction coefficients was only done for complex **3b**.

3.1. Absorption and emission spectra

The UV–Vis spectra of the MPc complexes with the respective mercaptoacetic acid and mercaptopropionic acid substituents in DMSO are shown in Fig. 1(a) and (b). The spectral data are listed in Table 1. The nature of the spectra in a (1:1) ethanol: 0.01 M NaOH solvent mixture are shown in Fig. 2 (a) and (b). The phthalocyanines are generally highly aggregated in both DMSO and aqueous media. Aggregation is usually depicted as a coplanar association of rings progressing from monomer to dimer and higher order complexes. Generally, the aggregates described in literature exhibit blue-shifted spectra with an absorption band near 630 nm, the so-called "H" aggregates [40]. Aggregation mainly occurs in aqueous media and addition of organic solvents or surfactants usually breaks up the aggregates. Fig. 1 shows that except for **3b**, all complexes are aggregated in DMSO. In aqueous media, Fig. 2, addition of ethanol breaks the aggregation only for the **3b** derivative (Fig. 2(b)), but the rest of the MPcs remain highly aggregated even upon addition of Triton X-100 (surfactant). As stated above, it is probable that the aggregation observed includes effects from hydrogen bonding since the MPc complexes have substituents with terminal carboxyl moieties and some of the complexes also have hydroxyl axial ligands (In^{3+}, Ga^{3+} and Si^{4+} complexes). The addition of organic solvents or surfactants should normally break the aggregates, resulting in monomeric species, however, the use of Triton X-100 and ethanol for the aqueous MPc solutions did not break the aggregates. Addition of CdTe QDs to the aggregated phthalocyanine complexes did

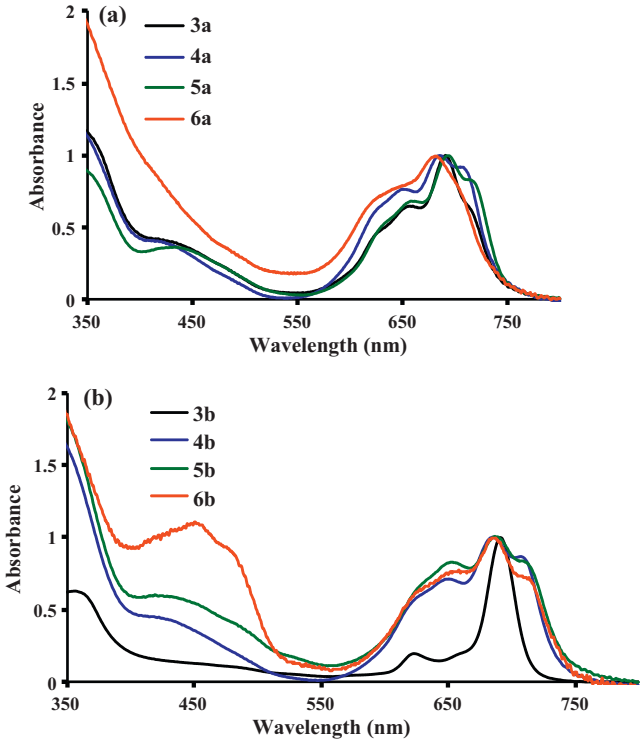

Fig. 1. Absorbance spectra of **3a**, **4a**, **5a** and **6a** in (a) and of **3b, 4b, 5b** and **6b** in (b) (in DMSO).

Table 1
Absorbance and fluorescence data for MPc complexes in DMSO, unless stated otherwise. Excitation at 620 nm.

MPc	Q band λ_{max} (nm)	Excitation λ_{max} (nm)	Emission λ_{max} (nm)	$\Phi_{F(MPc)}$
3a	658, 691, 714	717	723	0.02
4a	654, 687, 709	714	721	0.04
5a	643, 680, 705	717	716	0.03
6a	641, 684, 708	708	713	0.02
3b	692	695	706	0.13 0.14 (DMF) 0.19 (ethanol:water)
4b	653, 686, 712	715	722	0.07
5b	655, 687, 713	718	725	0.01
6b	652, 685, 715	717	724	0.04

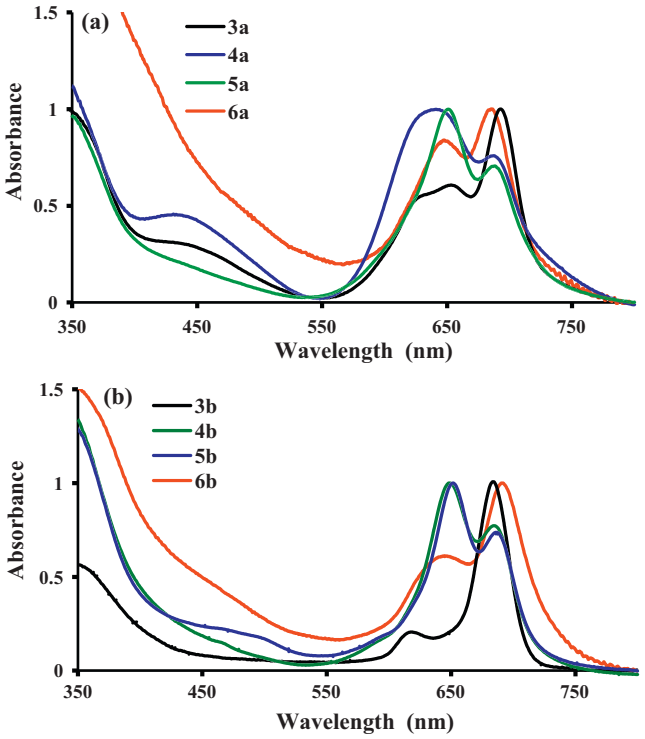

Fig. 2. Absorbance spectra of **3a**, **4a**, **5a** and **6a** in (a) and of **3b, 4b, 5b** and **6b** in (b) (in (1:1) ethanol:0.01 M NaOH solvent mixture).

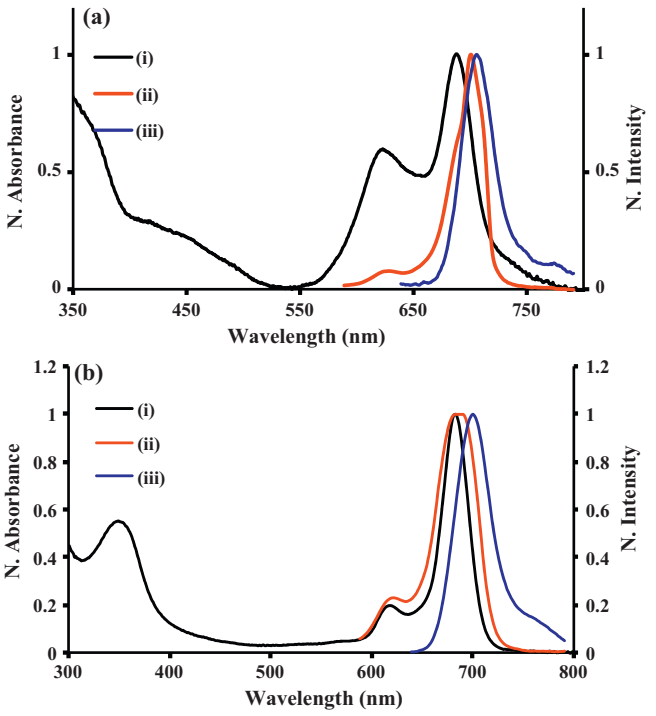

Fig. 4. Absorbance (i), excitation (ii) and emission (iii) spectra of (a) **3a** and (b) **3b** (in (1:1) ethanol:0.01 M NaOH solvent mixture, $\lambda_{excitation}$ = 620 nm).

not break the aggregates either, probably due to extensive hydrogen bonding. The absorbance, fluorescence emission and excitation spectra of the ZnPc complexes (**3a** and **3b** are shown in Figs. 3 and 4 in DMSO and a (1:1) ethanol:0.01 M NaOH solvent mixture, respectively. Aggregates are not known to fluoresce in MPc complexes, the observed broadening in the fluorescence spectrum of **3a** (representative all the complexes except **3b**) in DMSO (Fig. 3(a)) is probably due to the presence of isomers present in these tetra substituted complexes. For **3b** in DMSO, the emission spectrum is a mirror image of the excitation spectrum and both are broadened compared to the absorption spectrum. The emission of isomers will occur at wavelengths very close to one another, resulting in broadening. Apart from the broadening, the Q band maxima of the absorption and excitation spectra were very close to each other suggesting that nuclear configurations of the ground and excited states are similar and not affected by excitation for **3b**. Similar behaviour is observed in the (1:1) ethanol:0.01 M NaOH solvent mixture, Fig. 4 (for **3b**). The stokes shift observed for the MPcs were found to be within the range of those of MPc complexes [41].

The substituents employed both contain a terminal end with a carboxyl moiety thereby conferring a negative charge on to the MPc complexes that are reported on in this work. The QDs are also capped with MPA stabilizer groups that terminate in carboxyl moieties. The absorbance and emission spectra of the 4.1 nm QDs that were used in this work are shown in Fig. 5, with a typical broad absorption and narrow emission spectra. The absorbance spectra

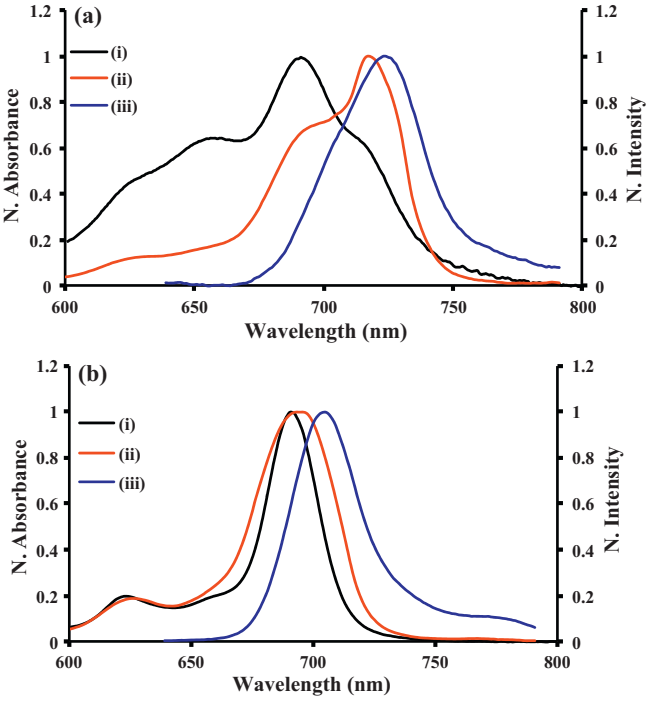

Fig. 3. Absorbance (i), excitation (ii) and emission (iii) spectra of (a) **3a** and (b) **3b** (in DMSO, $\lambda_{excitation}$ = 620 nm).

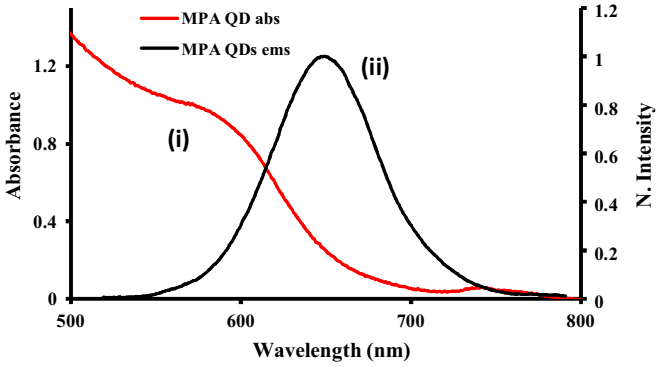

Fig. 5. Absorbance (i), and emission (ii) spectra of MPA QDs (1 mg/1 mL, in (1:1) ethanol:0.01 M NaOH solvent mixture, $\lambda_{excitation}$ = 500 nm).

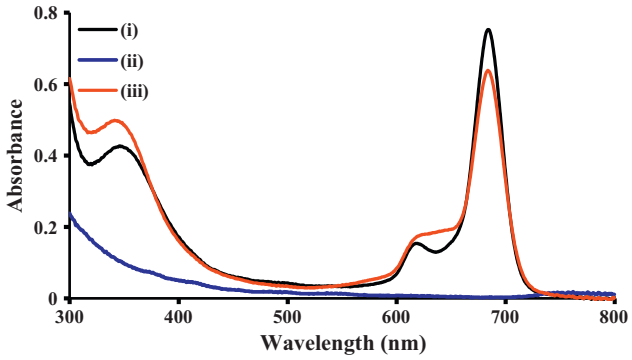

Fig. 6. Absorbance of (i) **3b** alone, (ii) MPA QDs alone and (iii) a mixture of **3b** and QDs. (in (1:1) ethanol:0.01 M NaOH solvent mixture).

Table 2
Fluorescence quantum yields of MPA QDs in the presence and absence of complex **3b**. Excitation at 500 nm.

Solvent	$\Phi_{F(QDs)}$	$\Phi^{Mix}_{F(QDs)}$
DMSO	0.32	0.19
DMF	0.21	0.10
ethanol:NaOH	0.22	0.15

of **3b** in the absence and presence of QDs is shown in Fig. 6 in aqueous media. There is only a slight broadening in the Q band and an increase in the intensity of the B band region due to absorption of the QDs. The Q band maxima remain the same in the presence and absence of QDs. The mode of interaction between the QDs and complex **3b** is most likely by adsorption.

3.2. Fluorescence parameters

3.2.1. Fluorescence quantum yields

Table 1 shows the fluorescence quantum yields (Φ_F) obtained by the use of equation 1. Φ_F values are low for all complexes compared to MPc complexes in general. The low Φ_F values are due to the highly aggregated nature of the complexes in solution. Complex **3b** which was not aggregated gave a value typical of Pc complexes [41] in different solvents, Table 1. For aggregated species, selection rules entail a large reduction in the fluorescence quantum yield, due to the increased rate of internal conversion from the first excited singlet state.

Φ_F values for quantum dots were 0.21, 0.22 and 0.32 in DMF, ethanol:0.01 M NaOH and DMSO, respectively, Table 2. In the presence of complex **3b**, the Φ_F values for QDs decreased, due to FRET, Table 2.

3.2.2. Fluorescence lifetimes

Fluorescence lifetime measurements were carried out and the results are shown in Table 3. The fluorescence lifetime measurements showed the QDs to exhibit a triexponential excitonic emission decay in all the solvents used (DMSO, DMF and (1:1) ethanol:0.01 M NaOH solvent mixture). Triexponential decay kinetics (Table 3) are quite common for CdTe QDs [42]. Studies to date have shown that the shorter lifetimes (fast decay component, τ_3) are mostly attributed to the carrier recombination within the core states but the much longer lifetimes (slow decay component, τ_1) usually involve carrier recombination processes in the surface defects sites [43–45]. The intermediate fluorescence lifetime component, (τ_2), is a result of radiative electron-hole recombination processes at the surface states [43]. There was a decrease for all lifetimes of QDs in the presence of MPcs in all solvents. The average amplitude weighted lifetimes (τ_{av}) were calculated and are shown in Table 3. The τ_{av} values (of QDs alone or in the presence of complex **3b**) in DMSO were observed to be the lowest for all the solvents used. The amplitude values (α) give the abundance of species with different lifetimes. α_1 values are higher for QDs alone than in the presence of **3b** in all solvents. In the ethanol: 0.01 M NaOH solvent mixture, α_1 (for quantum dots alone) was larger than α_2 or α_3 before addition of **3b**. On addition of **3b**, there is a decrease in α_1 and an increase in both α_2 and α_3 in the aqueous solvent mixture.

Time resolved emission spectroscopy (TRES) measurements were also carried out and the results of the MPc lifetime measurements are shown in Table 4. An example of TRES spectra is shown in Fig. 7(a) for aggregated complexes (using complex **4b** as an example). The inset in Fig. 7(a) shows the emission spectra of the monomeric (Fig. 7(a) inset (i)) and aggregated (Fig. 7(a) inset (ii)) forms of the Pc, with the aggregated specie of the Pc having shorter fluorescence lifetime τ_1 whereas the monomeric specie exhibits longer fluorescence lifetime τ_2. Almost all the MPcs studied indicated the same trend where the monomeric specie was in greater abundance except for **4a** where the aggregated specie was in greater abundance in solution. Thus the monomeric specie corresponds to the emission peak with higher intensity while the aggregated specie corresponds to the lower intensity peak in Fig. 7(a) (inset). As can be observed from the inset, the peak of higher intensity (monomeric specie at 722 nm) is also rather red shifted from the peak of lower intensity (aggregated specie at 712 nm). A comparison of the inset with the steady state emission spectrum of **4b** in Fig. 7(b) shows that the emission spectrum of monomeric specie shown in the inset (Fig. 7(a) inset (i)) lies at the

Table 4
Fluorescence lifetimes from TRES measurements of complexes **3a–6a** and **3b–6b** in DMSO.

Sample	[a]τ_1 (ns)	[b]α_1	[a]τ_2 (ns)	[b]α_2
3a	1.99 ± 0.03	0.35	3.75 ± 0.02	0.65
4a	2.27 ± 0.02	0.77	4.59 ± 0.04	0.23
5a	2.51 ± 0.06	0.38	4.97 ± 0.02	0.62
6a	1.95 ± 0.05	0.34	4.74 ± 0.02	0.66
3b	2.40 ± 0.02	0.28	3.73 ± 0.04	0.72
4b	1.99 ± 0.05	0.33	4.58 ± 0.05	0.67
5b	1.87 ± 0.06	0.28	4.35 ± 0.02	0.72
6b	2.09 ± 0.02	0.49	3.85 ± 0.02	0.51

[a] Fluorescence lifetimes at MPc emission.
[b] α Denotes the amplitude fraction.

Table 3
Fluorescence lifetime measurements from interactions between CdTe–MPA QDs and**3b** in DMSO, DMF and {(1:1) ethanol:0.01 M NaOH}.

Sample	[a]τ_1 (ns)	[b]α_1	[a]τ_2 (ns)	[b]α_2	[a]τ_3 (ns)	[b]α_3	τ_{av}
MPA QDs (DMSO)	30.86 ± 0.9	0.07	11.45 ± 0.1	0.43	2.05 ± 0.04	0.51	8.13
MPA QDs + **3b** (DMSO)	14.05 ± 0.1	0.03	2.41 ± 0.05	0.03	0.02 ± 0.001	0.95	0.51
MPA QDs (DMF)	32.57 ± 0.3	0.33	7.22 ± 0.1	0.46	1.72 ± 0.1	0.21	14.4
MPA QDs + **3b** (DMF)	9.02 ± 0.1	0.04	2.24 ± 0.03	0.17	0.44 ± 0.03	0.79	1.12
MPA QDs (EtOH:NaOH)	24.31 ± 0.2	0.63	17.58 ± 0.9	0.11	1.63 ± 0.1	0.26	17.68
MPA QDs + **3b** (EtOH:NaOH)	12.79 ± 0.07	0.27	2.60 ± 0.05	0.27	0.27 ± 0.02	0.46	4.28

[a] Fluorescence lifetimes at MPA-QD emission.
[b] α Denotes the amplitude fraction.

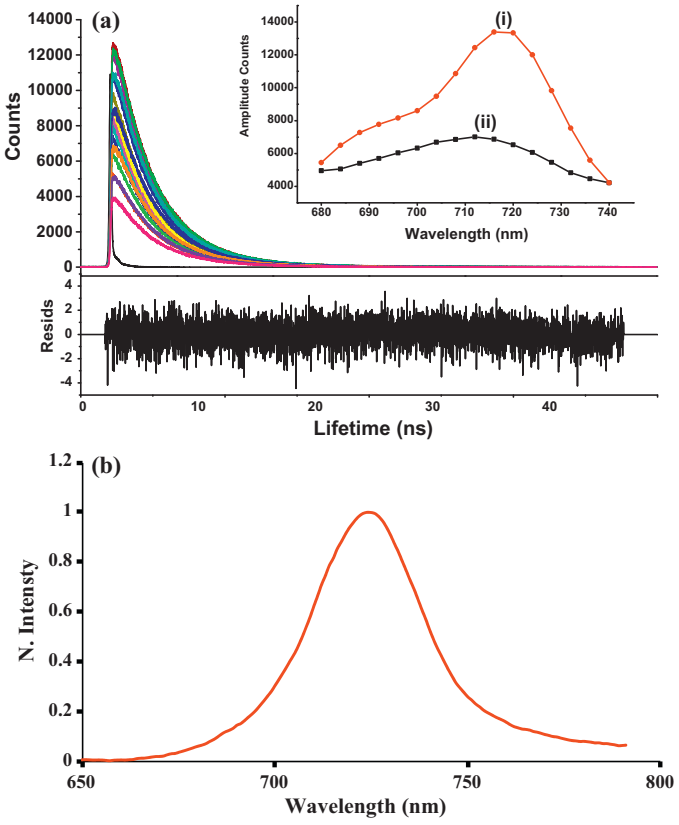

Fig. 7. (a)TRES Photoluminescence decay curves of **4b** in DMSO ($\lambda_{excitation}$ = 722 nm, measurements taken at the maximum of the exciton emission peak, $\tau_{1/e}$ = 4.58 ns): (i) long-lived species and (ii) short-lived species; and (b) steady state emission spectra of **4b**.

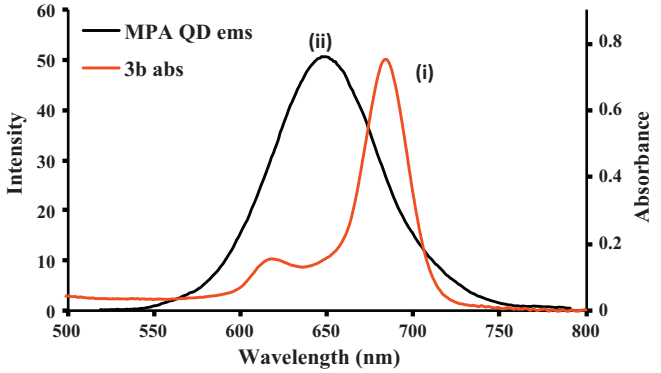

Fig. 8. (i) Absorbance (abs) of **3b**, and (ii) emission (ems) of MPA QDs. (in (1:1) ethanol:0.01 M NaOH solvent mixture, QDs $\lambda_{excitation}$ = 500 nm).

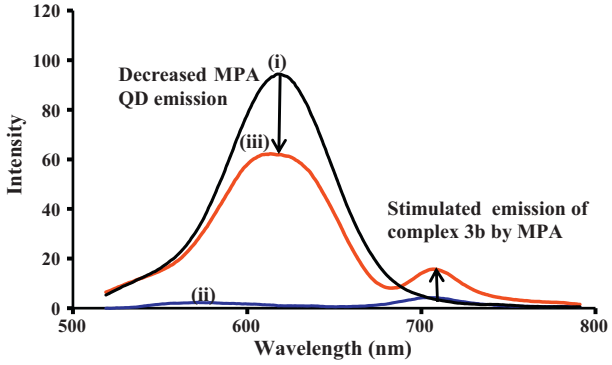

Fig. 9. Emission of (a) (i) QDs alone, (ii) **3b** alone and (iii) MPA QDs in the mixture with **3b** and for (b) ($\lambda_{excitation}$ = 500 nm, in (1:1) ethanol:0.01 M NaOH solvent mixture).

same wavelength as the emission maxima of the complex in steady state emission (722 nm as shown in Table 1).

3.2.3. *FRET studies*

FRET was observed between the CdTe MPA capped QDs of the size 4.1 nm and **3b** for the mixed in DMSO, DMF and in (1:1) ethanol:0.01 M NaOH solvent mixture. A good spectral overlap was observed between the donor (QD) emission spectra and the acceptor (**3b**) absorbance spectra and the overlap achieved in aqueous media as an example is shown in Fig. 8. The QDs were excited at 500 nm in the presence of the complex **3b**, where this complex does not absorb significantly, and hence has low or no fluorescence. Stimulated emission at 706 nm was observed due to FRET, Fig. 9, as judged by the increase in the emission peak at 722 nm when compared to complex **3b** alone.

The efficiency of FRET is known to be dependent on the spectral overlap term (*J*) estimated by overlapping QD emission with the absorbance of complex **3b** shown in Fig. 8. The overlap term *J* has varied units and for this work the units used were in cm^6 [29]. The PhotochemCAD program gives *J* units in cm^6 following the use of ε_{3b} in $M^{-1}\,cm^{-1}$ and λ in nm in Eq. (11). The Förster distance, R_0 (Å) which is the critical distance between the donor and the acceptor molecule fluorophores for which efficiency of energy transfer is 50% [46,47] is also obtained from PhotochemCAD, while the center-to-center separation distance (*r*, Å) between donor and acceptor fluorophores is obtained from the use of Eq. (9) and are listed in Table 5.

The values for J are generally of the order $10^{-14}\,cm^6$ for molecules that are porphyrin based. In this work the values obtained were also of the order $10^{-14}\,cm^6$ for the overlap between the MPA capped QDs and complex **3b** as shown in Table 5. The relatively high value of *J* is an indication of good spectral overlap of the emission spectrum of the donor and the absorption spectrum of the acceptor. An estimation of a donor–acceptor oscillator match can be deduced from *J* values. It is well established that FRET only takes place when *r* values are within the range of 2–10 nm [16,29,47]. The values of *r* calculated from Eq. (9) for QDs: complex **3b** mixtures were 3.99 nm, 3.37 nm and 3.74 nm in DMSO, DMF, and aqueous media, respectively. As shown in Table 5, the *r* values were fairly small suggesting that the MPc complex is in close proximity to the donor (QD's) and thus there should be an ease of non-radiative energy transfer from the excited CdTe MPA QDs to **3b** molecules. A comparison of FRET efficiencies for **3b** in a mixture with QDs obtained by TCSPC measurements and steady state fluorescence

Table 5
Energy transfer parameters for TMPAZnPc–CdTe MPA QD interactions.

MPc and MPA–CdTe QDs	$J/10^{14}\,cm^6$	$R_0/10^{10}$ m	$r/10^{10}$ m	[a]Eff	[b]Eff
TMPAZnPc (**3b**) + MPA QDs (DMSO)	7.1	37.7	39.9	0.42	0.94
TMPAZnPc (**3b**) + MPA QDs (DMF)	7.0	35.6	33.7	0.58	0.92
TMPAZnPc (**3b**) + MPA QDs (EtOH: 0.01M NaOH (1:1))	3.4	33	37.4	0.32	0.75

[a] FRET efficiencies from steady state fluorescence spectra.
[b] FRET efficiencies from TCSPC lifetime measurements.

Table 6
Photophysical parameters for **3b** alone or in the presence of QDs.

Sample	Solvent	$\Phi_{T(MPc)}$	$\tau_{T(MPc)}$/μs	Φ_{IC}	Φ_{Δ}	S_{Δ}
3b	DMSO	0.88	230	~0	0.86	0.98
3b + QD	DMSO	0.94	210			
3b	DMF	0.61	320	0.25	0.60	0.98
3b + QD	DMF	0.67	180			
3b	ethanol:NaOH	0.63	13	0.18	0.33	0.52
3b + QD	ethanol:NaOH	0.80	188			

was carried out. These efficiencies were calculated using Eqs. (8) and (7), respectively. The results from steady state fluorescence show the FRET efficiency to be highest in DMF (*Eff* = 58%) while the TCSPC results show the FRET efficiency to be highest in DMSO (*Eff* = 94%) followed by that in DMF (*Eff* = 92%), Table 5. The two sets of results show FRET efficiency values that are far off from each other but they both follow the same trend. The lifetime measurements are very sensitive and so the contribution of other processes such as dynamic or static quenching would thus lower the fluorescent lifetimes further even in the event of FRET. As a result the efficiency obtained is not a true reflection of the FRET process only. Although the intensity values from steady state fluorescence measurements are also affected by similar quenching effects, they are not as sensitive to quenching as the lifetime measurements [29,48].

3.3. Triplet state quantum yields (Φ_T) and lifetime (τ_T) studies

The Φ_T values were obtained by the use of Eq. (3). These values give a measure of the fraction absorbing molecules that undergo intersystem crossing (ISC) to the triplet state. In Table 6 a variation of Φ_T values of the **3b** complex in the absence and presence (in DMSO, DMF and aqueous media) of the QDs is shown. The Φ_T values of complex **3b** were reasonably high in the presence and the absence of QDs. This serves as an indication that a considerable number of the molecules of the complexes undergo intersystem crossing to the triplet state. An increase of the Φ_T values in the presence of the quantum dots was observed for **3b**. This observation is attributed to the heavy Cd and Te atoms of QDs which encourage intersystem crossing (to the triplet state) of the MPc complex. An increase of the Φ_T values in the presence of QDs has been previously reported by our group [25,49].

The triplet lifetime (τ_T) values of the complex **3b** in the presence of QDs were generally lower than the τ_T values for the complex **3b** alone, corresponding to increased Φ_T values. However, in the (1:1) ethanol:0.01 M NaOH solvent mixture, the τ_T values increased in the presence of QDs as has been observed in other studies in aqueous media [50].

The Φ_{IC} values were obtained by employing Eq. (4). As shown in Table 6, the values of Φ_{IC} for complex **3b** were rather low indicating that radiationless transitions do not play an important role in the deactivation of the excited state. The combined effect of deactivation of the excited state by radiationless transitions and the high Φ_T values account for the low Φ_F values obtained for **3b**.

3.4. Singlet oxygen quantum yields

The singlet oxygen quantum yield Φ_{Δ} is a measure of singlet oxygen generation. Φ_{Δ} values were obtained using Eq. (5). Interaction of the triplet state of a photosensitizer and the ground state molecular (triplet) oxygen $^3O_2(^3\Sigma_g^-)$ allows for the production of singlet oxygen. The efficiency of singlet oxygen generation depends on the triplet state quantum yield Φ_T and the triplet state lifetime τ_T. Relatively high values of Φ_T and τ_T result in elevated Φ_{Δ} values. This is due to increased molecular interactions between the photosensitizer in its triplet state and the ground state oxygen $^3O_2(^3\Sigma_g^-)$ to produce more singlet oxygen $^1O_2(^1\Sigma_g^-)$. Table 6 shows that the Φ_T values for **3b** are relatively high in all the three solvents used for the study and so high values of Φ_{Δ} were also anticipated. The corresponding values of Φ_{Δ} as shown in Table 6 were high: Φ_{Δ} = 0.86 (DMSO), Φ_{Δ} = 0.60 (DMF) and Φ_{Δ} = 0.33 ((1:1) ethanol:0.01 M NaOH solvent mixture). The lowest value was observed for **3b** in aqueous media.

Solvents (such as water) that absorb around 1100 nm (triplet energy level of Pcs) and around 1270 nm (singlet oxygen energy level) quench the triplet state of the MPc derivative as well as singlet oxygen [27], hence the low value of Φ_{Δ} in aqueous media is not surprising.

The values of the fraction of the excited triplet state quenched by ground state molecular oxygen (S_{Δ}) were calculated using Eq. (6). S_{Δ} values are a reflection of the efficiency of energy transfer from the triplet state of the MPc complexes to the ground state of molecular oxygen. Values of S_{Δ} close to unity are an indication of a high efficiency of energy transfer. As shown in Table 6, the S_{Δ} values for **3b** in DMSO and DMF are close to unity while in aqueous media the S_{Δ} value is mediocre.

4. Conclusions

The synthesis and characterization of water soluble Zn^{2+}, In^{3+}, Ga^{3+} and Si^{4+} phthalocyanine complexes was carried out successfully. The MPcs were found to have intense aggregation effects which hindered the study of the photophysical and photochemical properties except for **3b**. FRET was observed for **3b** in the presence of MPA QDs in all the solvents used for the study. The center-to-center distance between the donor and acceptor fluorophores was found to be quite small ~5 nm thus facilitating FRET.

Acknowledgements

This work was supported by the Department of Science and Technology (DST) and National Research Foundation (NRF), South Africa through DST/NRF South African Research Chairs Initiative for Professor of Medicinal Chemistry and Nanotechnology as well as Rhodes University and Medical Research Council of South Africa. S.M. thanks DAAD foundation for a scholarship.

References

[1] I. Okura, Photosensitization of Porphyrins and Phthalocyanines, Gordon and Breach Science Publishers, Amsteldijk, The Netherlands, 2001, pp. 151–213.
[2] E. Ben-Hur, W.S. Chan, in: K.M. Kadish, K.M. Smith, R. Guilard (Eds.), Porphyrin Handbook, Phthalocyanine Properties and Materials, vol. 19, Academic Press, New York., 2003 (Chapter 117).
[3] R. Bonnet, Chemical Aspects of Photodynamic Therapy, Gordon and Breach Science Publishers, Amsterdam, 2000.
[4] E.A. Lukyanets, V.N. Nemykin, J. Porphyrins Phthalocyanines 14 (2010) 1–40.
[5] V.N. Nemykin, E.A. Lukyanets, ARKIVOC i (2010) 136–208.
[6] S. Moeno, T. Nyokong, J. Photochem. Photobiol. A: Chem. 203 (2009) 204–210.
[7] A.C. Tedesco, J.C.G. Rotta, C.N. Lunardi, Curr. Org. Chem. 7 (2003) 187–196.
[8] K. Ishii, N. Kobayashi, in: K.M. Kadish, K.M. Smith, R. Guilard (Eds.), The Porphyrin Handbook, vol. 16, Elsevier, 2003 (Chapter 1).
[9] J.D. Spikes, J. Photochem. Photobiol. B 6 (1990) 259–274.
[10] C.M. Allen, W.M. Sharman, J.E. Van Lier, J. Porphyrins Phthalocyanines 5 (2001) 161–169.
[11] I.J. Macdonald, T.J. Dougherty, J. Porphyrins Phthalocyanines 5 (2001) 105–129.
[12] A.L. Rogach, L. Katsikas, A. Kornowski, D. Su, A. Eychmüller, H. Weller, Ber Bunsenges, Phys. Chem. 100 (1996) 1772–1778.
[13] A.C.S. Samia, S. Dayal, C. Burda, Photochem. Photobiol. 82 (2006) 617–625.
[14] E.R. Goldman, I.L. Medintz, H. Mattoussi, Anal. Bioanal. Chem. 384 (2006) 560–563.
[15] A.L. Rogach, Mat. Sci. Eng. B 69–70 (2000) 435–440.
[16] L. Stryer, Annu. Rev. Biochem. 47 (1978) 819–846.
[17] L. Lankiewicz, J. Malicka, W. Wiczk, Acta Biol. Pol. 44 (1997) 477–489.
[18] D. Sokol, X. Zhang, P. Lu, A. Gewirtz, Proc. Natl. Acad. Sci. U. S. A. 95 (1998) 11538–11543.
[19] S. Dayal, C. Burda, J. Am. Chem. Soc. 129 (2007) 7977–7981.
[20] M. Idowu, T. Nyokong, J. Lumin. 129 (2009) 356–362.
[21] S. Moeno, T. Nyokong, J. Photochem. Photobiol. A: Chem. 201 (2009) 228–236.
[22] S. Moeno, M. Idowu, T. Nyokong, Inorg. Chim. Acta 361 (2008) 2950–2956.

[23] F. Dumoulin, M. Durmuş, V. Ahsen, T. Nyokong, Coord. Chem. Rev. 254 (2010) 2792–2847, references therein.
[24] N. Gaponik, V.D. Talapin, K. Hoppe, E.V. Shevchenko, A. Kornowski, A. Eychmuller, H. Weller, J. Phys. Chem. B 106 (2002) 7177–7185.
[25] S. Moeno, E. Antunes, S. Khene, C. Litwinski, T. Nyokong, Dalton Trans. 39 (2010) 3460–3471.
[26] S. Fery-Forgues, D. Lavabre, J. Chem. Ed. 76 (1999) 1260–1264.
[27] A. Ogunsipe, J.-Y. Chen, T. Nyokong, New J. Chem. 28 (2004) 822–827.
[28] R.F. Kubin, A.N. Fletcher, J. Lumin. 27 (1982) 455–462.
[29] J.R. Lakowiecz, Principles of Fluorescence Spectroscopy, 2nd ed., Kluwer Academic/Plenum Publishers, New York, 1999.
[30] T.H. Tran-Thi, C. Desforge, C. Thiec, J. Phys. Chem. 93 (1989) 1226–1233.
[31] A. Harriman, M.C. Richoux, J. Chem. Soc. Faraday Trans. II 76 (1980) 1618–1626.
[32] P. Kubat, J. Mosinger, J. Photochem. Photobiol. A96 (1996) 93–97.
[33] J. Kossanyi, D. Chahraoui, Int. J. Photoenergy 2 (2000) 9–15.
[34] S. Maree, T. Nyokong, J. Porphyrins Phthalocyanines 5 (2002) 782–792.
[35] A. Ogunsipe, D. Maree, T. Nyokong, J. Mol. Struct. 650 (2003) 131–140.
[36] N. Kuznetsova, N. Gretsova, E. Kalmykova, E. Makarova, S. Dashkevich, V. Negrimovskii, O. Kaliya, E. Lukyanets, Russ. J. Gen. Chem. 70 (2000) 133–140.
[37] N. Kuznetsova, E. Makarova, S. Dashkevich, N. Gretsova, E. Kalmykova, V. Negrimovsky, O. Kaliya, E. Luk'yanets, Obshch. Khim. 70 (2000) 140–148.
[38] F. Wilkinson, W.P. Helman, A.B. Ross, J. Phys. Chem. Ref. Data 22 (1993) 113–262.
[39] H. Du, R.A. Fuh, J. Li, L.A. Corkan, J.S. Lindsey, Photochem. Photobiol. 68 (1998) 141–142.
[40] H. Engelkamp, R.J.M. Nolte, J. Porphyrins Phthalocyanines 4 (2000) 454–459.
[41] T. Nyokong, Coord. Chem. Rev. 251 (2007) 1707–1722.
[42] M. Sanz, A. Miguel, C. Duarte, M. Luis, L. Marzán, A. Douhal, J. Photochem. Photobiol. A: Chem. 196 (2008) 51–58.
[43] M. Lunz, A.L. Bradley, J. Phys. Chem. C 113 (2009) 3084–3088.
[44] J. Zhang, X. Wang, M. Xiao, Opt. Lett. 27 (2002) 1253–1255.
[45] X. Wang, L. Qu, J. Zhang, X. Peng, M. Xiao, Nanoletter 3 (2003) 1103–1106.
[46] J.S. Hsiao, B.P. Krueger, R.W. Wagner, T.E. Johnson, J.K. Delaney, D.C. Mauzerall, G.R. Fleming, J.S. Lindsey, D.F. Bocian, R.J. Donohoe, J. Am. Chem. Soc. 118 (1996) 11181–11193.
[47] T. Forster, Disc. Far. Soc. 27 (1959) 7–17.
[48] C. Biskup, T. Zimmer, L. Kelbauskas, B. Hoffmann, N. Klöcker, W. Becker, A. Bergmann, Microsc. Res. Technol. 70 (2007) 442–451.
[49] J. Ma, J.Y. Chen, M. Idowu, T. Nyokong, J. Phys. Chem. B 112 (2008) 4465–4469.
[50] M. Idowu, J.-Y. Chen, T. Nyokong, New J. Chem. 32 (2008) 290–296.